

## CONSTRUCTION OF AN EVAPORATION SYSTEM FOR FILM DEPOSITION VIA RESISTIVE AND ELECTRON BEAM SOURCES

F.S. De Vicente<sup>1,\*</sup>; E.A.A. Rubo<sup>2</sup>; M. Siu Li<sup>1</sup>

<sup>1</sup>Instituto de Física de São Carlos, USP, CP 369, São Carlos, 13560-970-SP, Brasil

<sup>2</sup>Departamento de Física, UNESP, CP 473, Bauru, 17033-360-SP, Brasil

Received: July 30, 2003; Revised: June 8, 2004

Keywords: construction, evaporation system, vacuum deposition.

### ABSTRACT

*An evaporation system with both resistive and electron beam sources and also specific accessories for optimized film deposition in vacuum has been designed and built. The aim for the construction of the apparatus was to produce films with thickness from few hundreds of nanometers up to tenths of microns, starting from materials among a wide range of evaporation temperatures. This system presents low cost as also easy maintenance compared with commercial systems for films deposition.*

### 1. INTRODUCTION

In the last decades much effort has been realized in the study of materials and techniques intended for miniaturized devices production in favor of technological applications [1,2].

A large percentage of this branch is due to suitable ways of thin film fabrication and its use in the production of such compact devices [3,4]. In addition, we can cite some important devices developed by using film deposition, as well as, ultra-compact diode lasers [5], random access memories (RAM) [6], photovoltaic cells [7], and also CDs and DVDs [8].

For each material to be deposited in film form is necessary take in account the more appropriated process for a rapid and successful production.

The process of films deposition can be divided in two main categories: 1) The Physical Processes or Physical Vapour Deposition (PVD) [9,10], which include Resistive and Electron Beam evaporation, and also Sputtering; and 2) Chemical Processes [11,12], consisting of Chemical Vapour Deposition (CVD), Langmuir-Blodgett and Sol-Gel.

The two last techniques involve polymerisation of inorganic precursors such as inorganic salts dissolved in organic solvents and deposited by dip coating or spin coating.

Particularly, the PVD processes allow the production of films from a wide range of materials, such as, metallic, dielectrics and semiconductors with relatively low deposition times [13,14]. This led us to decide on the construction of an evaporation system with thermal sources for films deposition.

The present work presents the design, construction and characterization of an evaporation system with resistive and electron beam sources for vacuum film deposition.

### 2. EVAPORATION SYSTEM DESCRIPTION

The evaporation system is described in two parts, which consist of the Evaporation Chamber and Specific Accessories. The specific accessories correspond to the thickness gauge, substrate heater, Quartz windows, and the motor-driven chamber elevator, described detailed in the section 2.2. All the parts of the evaporation system were mounted on a metallic board constructed with rectangular steel tubes. The metallic board possess four feet with level adjust and also four wheels for transportation.

#### 2.1. Evaporation Chamber

The Figure 1 shows an overview of the evaporation system as well the evaporation chamber, resistive source, electron beam gun, vacuum system, and the motor-driven chamber elevator, fig 1-a to 1-e, respectively.

The evaporation chamber was made in stainless steel 304, with internal volume of 103 liters and has five glass windows for evaporation monitoring. The chamber base is also in stainless steel with thickness of 23 mm and 645 mm in diameter.

In the Figure 2 is presented the side and top view of the chamber base with the apertures disposition used in the mounting, with the principal dimensions in millimeters.

Also some specific accessories and features are detailed in the figure 2 as the thickness gauge, heater and substrate support, electron beam gun front view, Quartz optical windows, gas-injection valve, Diffusion pump aperture, and electron beam gun top view (fig. 2-a to 2-g, respectively).

#### 2.1.1. Resistive Source

The resistive source for evaporation contains three pairs of ceramic-isolated copper electrodes with vacuum connectors (FT-150/133) and flanges from Duniway Stockroom Corporation. The electrodes were mounted on the base for deposition of materials using crucibles such as Ta, Mo, Nb, and,

\* vicente@if.sc.usp.br

W. The resistive power supply is a Varivolt from 0-220 V with current up to 100 A.

The Figure 3 presents one pair of electrodes mounted on the chamber base.

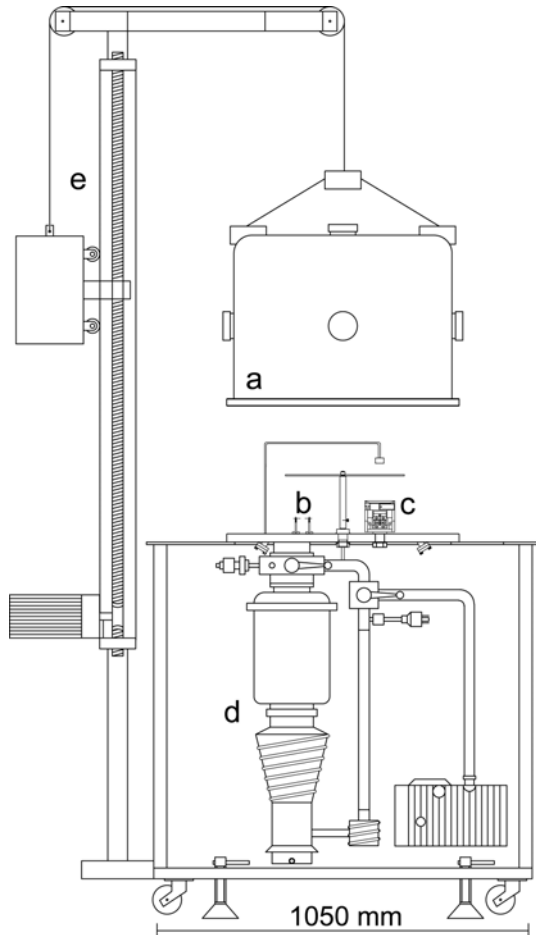


**Figure 1 – Overview of the evaporation system. a) evaporation chamber, b) resistive source, c) electron beam gun, d) vacuum system, e) motor-driven chamber elevator.**

The crucibles used in the resistive evaporation can be in the boat, foil, or wire form to be fixed by screws in the crucible supports, depending of the materials to be deposited. The resistive source provides evaporation temperatures up to 1000 °C with crucible such as Tantalum (Ta) and Tungsten (W).

### 2.1.2. Electron Beam Source

An electron beam gun from Telemark-231 that operates from 4-10 kV and maximum electron beam current of 500 mA was mounted in the chamber base [15]. The Figure 4 shows the top and side views of the electron beam gun. The nucleus of the electron beam gun is made of copper and refrigerated by water that flows into the central part of the electron beam gun through the in-out connectors (fig 4-a)

and also into the crucibles support (fig 4-b) by the in-out connectors (fig 4-d). Up to four different materials can be deposited independently onto substrates via electron beam source by a crucible rotation system. The rotation of the four-crucible support is controlled by a pass-motor as shows the figure 4-c.

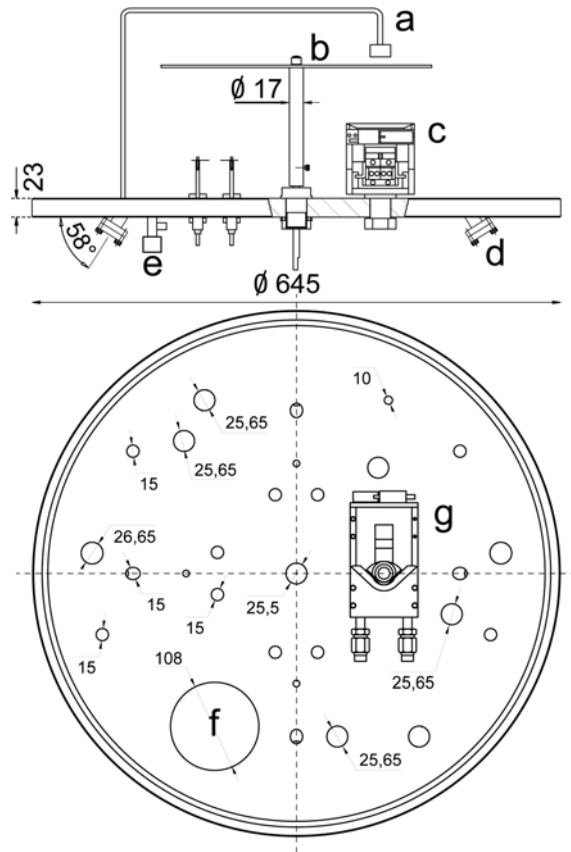


**Figure 2 – Chamber base. (Up) Side view: a) thickness gauge, b) heater and substrate support, c) electron beam gun front view, d) Quartz optical windows, e) gas-injection valve; (Down) Top view: f) diffusion-pump aperture, g) electron beam gun top view. Also are shown the apertures disposition used in the mounting (dimensions in millimeters).**

The electron beam is generated in the emitter part (fig 4-e), composed of a Tungsten filament supplied with 0-12 V and 0-3 A, placed between two plates (anode and cathode) supplied with 4 up to 10 kV for acceleration of the electrons emitted by the heated Tungsten filament. Two magnetic lateral plates of the gun lead the electron beam to reach the crucibles by a circular trajectory.

The electron beam gun power supply is composed by a voltage module and a current module connected to a control unit [15]. In the control unit is possible to adjust accurately the high voltage that accelerates the electrons as also the beam current emitted by the filament.

A X-Y sweep module is also present in the control unit, which permits to set a scan pattern and the position of the electron beam on the target to be evaporated.

## 2.2. Specific Accessories

The specific accessories correspond to the thickness gauge, Quartz windows for films *in-situ* characterization, and Chamber elevator mounted in the system as previously shown (figs. 1 and 2), and also the substrate heater, described as follow.

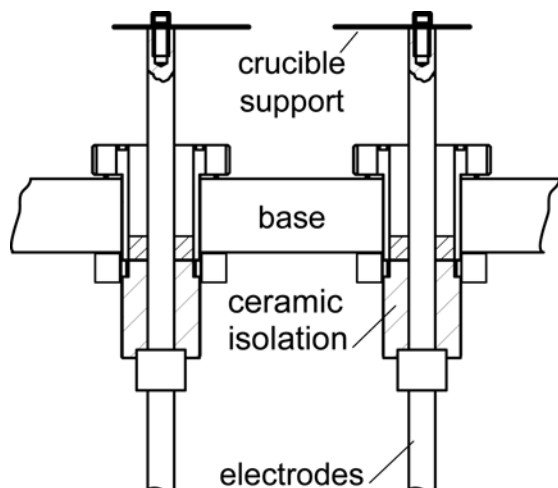


Figure 3 – Electrodes used for resistive evaporation, mounted on the chamber base.

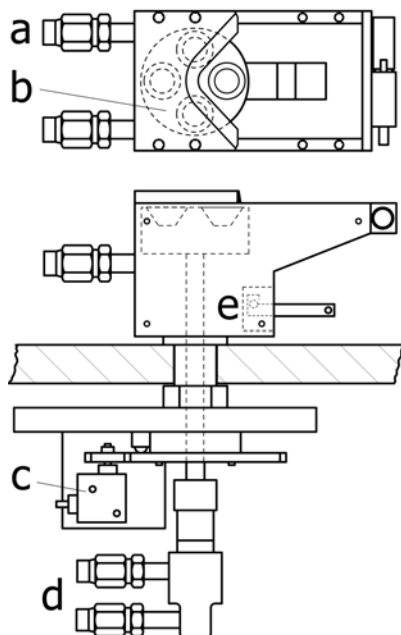


Figure 4 – Electron Beam Gun; (Up) Top view: a) Water refrigeration in-out connectors, b) Four crucible support; (Down) Side view: c) Pass-motor to crucible support rotation, d) Crucibles water refrigeration connectors, e) Electron beam emitter part.

### 2.2.1. Thickness Gauge

The thickness gauge is based on a quartz crystal oscillator connected to a digital display module from Sycon Instruments STM-100 [16]. The quartz crystal sensor was mounted in such manner to stay as close as possible to the heater and substrates support, as shown in figure 2-a.

A digital display module shows the thickness measured by the sensor in angstroms, as also the deposition rate in angstroms per second. The digital display module permits to configure some parameters as density of the material, final thickness desired, etc.

### 2.2.2. Substrate Heater

The substrate heater was mounted in a stainless steel cup with ~60 mm in diameter and 10 mm in depth with 0.7 mm Tantalum wire, braided on ceramic isolators. The heater is disposed above the resistive or electron beam source, on the support as shown in figure 2-b and supplied by a Varivolt (0-200V, 10 A) through the same connectors used for resistive evaporation (FT-150/133).

Figure 5 presents the side and bottom view of the substrate heater. The side view (left) shows the mounting sequence of the heater, which corresponds to the support of the ceramic isolators and Tantalum wire, base of the heater, view of as the substrates are fixed, and substrates support, (Fig 5-a to 5-d) respectively. The bottom view (right) shows how the Tantalum wire was braided on the ceramic isolators fixed in the stainless steel cup, and also the detail of the substrates support.

Using this setup was possible to range the substrates temperature from RT up to 800°C. The temperature is measured by a thermocouple wire fixed in the base of the heater.

### 2.2.3. Quartz Windows

Four Quartz windows (VP-133-075 from Duniway Stockroom Corporation) were symmetric disposed in the bottom of the chamber base (see figure 2-d) for *in-situ* characterization of the films as also laser irradiation during the deposition process. The windows were mounted with inclination of 58°, which permits a beam of light to access directly the substrates.

### 2.2.4. Chamber Elevator

A motor-driven chamber elevator was necessary due to the weight of the stainless steel chamber and also to assist the system operation. The elevator consists of a simple gate opening system with remote control that was adapted in the board of the evaporation system. The elevator was mounted in the vertical position and connected to the chamber through a steel cable as shown in Figure 1-e.

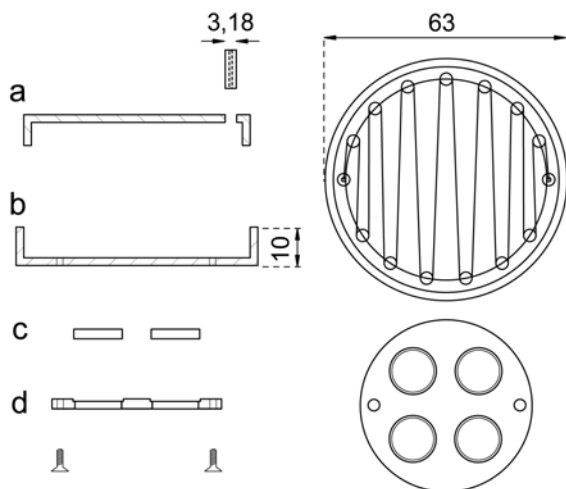


**Figure 5 – Substrates Heater (left: side view and right: bottom view). a) Support of the ceramic isolators and Tantalum wire, b) base of the heater, c) view of as the substrates are fixed, d) substrates support. (dimensions in millimeters).**

### 3. EXPERIMENTAL RESULTS

In this section we give a brief description of some results published elsewhere [17-21], obtained in the constructed evaporation system for materials deposited by both resistive and electron beam sources. A short comparison is made with results presented in the literature.

Ti<sup>+</sup> doped KCl, KBr and KI crystalline films were deposited by resistive and electron beam sources, presenting high dopant incorporation and excellent optical properties [17]. For comparison, it is important to note that a KCl single crystal doped with 1.0 mol % of TiCl presents a concentration of 10<sup>18</sup> cm<sup>-3</sup> of Ti<sup>+</sup> ions, while for the same doping conditions films of KCl:Ti<sup>+</sup> obtained by thermal evaporation achieve concentrations of 10<sup>21</sup> cm<sup>-3</sup> of Ti<sup>+</sup> ions [22]. Azobenzene DR13 dye films with 1.0 μm in thickness were prepared by resistive source with crucible temperature slowly increased up to 80 °C and RT substrate temperature [18]. Several techniques have been used to produce films from azobenzene-containing materials, such as spin-coating [23], electrostatically assembled layer-by-layer (LBL) [24] and Langmuir-Blodgett (LB) [25] methods, therefore these techniques are only suitable for polymeric films and do not allow the fabrication of films from small molecules (or monomers). This difficulty was circumvented by using physical vapour deposition (PVD), in which the deposited films maintain the precursor chemical characteristics [18,26].

Crystalline ZrO<sub>2</sub>:Er<sup>3+</sup> films with good optical quality up to 5.0 μm were obtained by electron beam evaporation, deposited onto quartz substrates submitted at 400°C [19]. Deposition rates of 5.0 Å/sec were achieved for this material, monitored by the quartz crystal oscillator. Tantalum cruci-

bles were used to support the high evaporation temperature of the ZrO<sub>2</sub> (2100°C at 10<sup>-6</sup> Torr).

It was observed that the substrate temperature is a determinant factor in the structure and crystallinity of the ZrO<sub>2</sub>:Er<sup>3+</sup> deposited films. Amorphous rare-earth doped Zirconia films were obtained and reported by other authors [27,28], however we observed that is possible to control the phase of ZrO<sub>2</sub> films during the deposition process by heating the substrate. Although the cubic phase in bulk Zirconia exists only at temperatures beyond 2300 °C as also at high dopant concentrations (>10 mol.%) [29], in our case the ZrO<sub>2</sub>:Er<sup>3+</sup> films deposited with substrate heated at 400°C presented only crystalline cubic phase [19].

Homogeneous amorphous films with photoinduced effects were successfully produced by electron beam evaporation, starting from Polyphosphate Glasses, with deposition rates of 100 Å/sec and up to 10 μm in thickness [20].

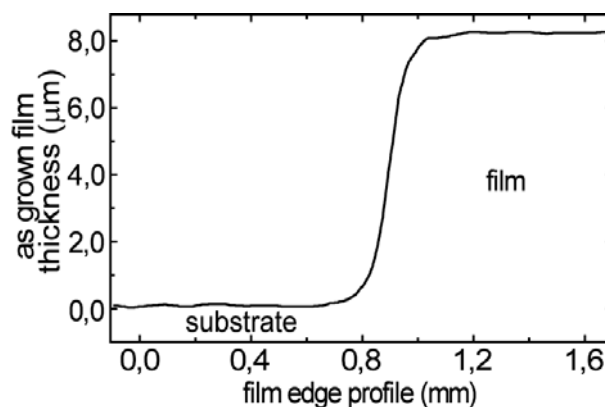


**Figure 6 – Thickness and film edge profile of the ~ 8μm amorphous Polyphosphate films deposited by electron beam evaporation.**

The thickness of the amorphous Polyphosphate films was determined by a profiler Talystep Rank Taylor Hobson as presents the Figure 6. The Figure 7 shows a SEM image of the surface and the edge detail of an ~ 8.0 μm Polyphosphate film.

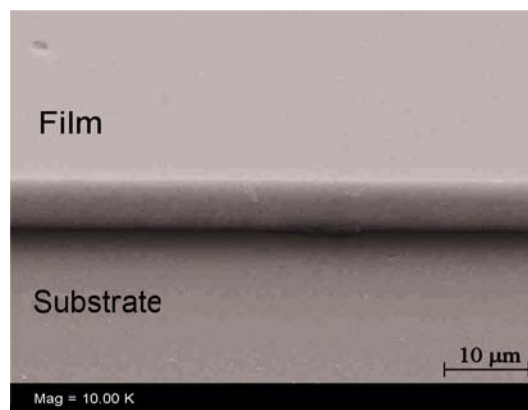


**Figure 7 – SEM image of the surface and the edge detail of an ~ 8.0 μm Polyphosphate film deposited by electron beam.**

Recently polycrystalline films ( $\sim 400$  nm-thickness) of  $\text{LaNiO}_3$  were obtained by electron beam evaporation, on single-crystal  $\text{PtTiSi}$  substrates heated at  $700^\circ\text{C}$  during the deposition process [21]. The Figure 8 shows the X-ray diffraction pattern of  $\text{LaNiO}_3$  films produced by electron beam evaporation (fig 8-a) and spin coating technique (fig. 8-b).

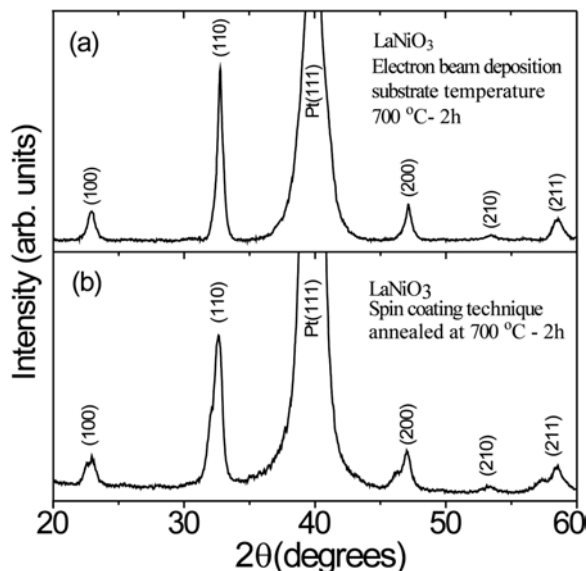


**Figure 8 – X-ray diffraction pattern of  $\text{LaNiO}_3$  films produced by a) electron beam evaporation, and b) spin coating technique.**

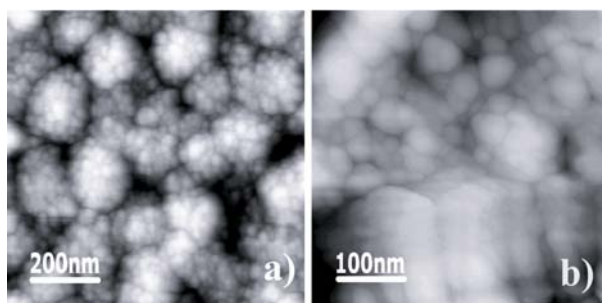


**Figure 9 – AFM images showing the surface morphology of  $\text{LaNiO}_3$  films produced by a) electron beam evaporation, and b) spin coating technique.**

The  $\text{LaNiO}_3$  films deposited by electron beam evaporation on  $\text{PtTiSi}$  substrates heated at  $700^\circ\text{C}$  during deposition were obtained in a more crystalline phase (sharper XRD peaks) with cubic structure when compared with the films deposited by spin coating, which presented a mixed rhombohedral and cubic structure (see fig 8-a and 8-b). Also the  $\text{LaNiO}_3$  films deposited by electron beam evaporation on  $\text{PtTiSi}$  substrates heated at  $700^\circ\text{C}$  have smooth surface morphology than those prepared by spin coating as observed by AFM images presented in Figure 9. The polycrystalline structure of the  $\text{LaNiO}_3$  thin films obtained in this work is in sharp contrast with the results reported by Tseng et al. [30] that observed (110) oriented films. In addition, Kin et al. [31]

obtained a single  $\text{LaNiO}_3$  phase that was formed by pulsed laser deposition with the (00 $l$ ) planes predominantly parallel to the substrates surface.

The films produced in the constructed evaporation system were mainly characterized by X-ray diffraction, Visible and FTIR Optical Absorption, Raman Scattering and Atomic Force Microscopy.

#### 4. CONCLUSION

In this work we presented the design and construction details of an Evaporation System with resistive and electron beam sources for vacuum film deposition. This system presents low cost and easy maintenance compared with commercial systems for films deposition. Films with thickness ranging from 400 nm up to 10  $\mu\text{m}$  have been produced starting from materials within a wide range of fusion temperatures, by using both resistive and electron beam sources. These films present excellent quality and properties that have been recently explored in our research [17-21].

#### 5. ACKNOWLEDGEMENTS

The authors acknowledge the financial support received from the Brazilian Institutions, FAPESP, CNPq, CAPES, and FINEP. We also thanks to Dr. Carlos Alberto Baldan from Faculdade de Engenharia Química de Lorena, for providing the Tantalum and Niobium crucibles used for electron beam evaporation, Profa. Dra. Ligia de Oliveira and Prof. Dr. Milton Ferreira de Souza by the collaboration and fruitfully discussions, and also to the designer Samuel Alvarez and technicians Carlos N. Gonçalves, Celso E. Ferri, and Evaldo J. P. de Carvalho, from the mechanics factory of Instituto de Física de São Carlos-USP.

#### 6. REFERENCES

1. HÜLSENBERG, D. *Microelectronics Journal* 28 (1997) 419.
2. MAIRAJ, A.K.; RIZIOTIS, C.; CHARDON, A.M.; SMITH, P.G.R.; SHEPHERD, D.P.; HEWAK, D.W. *Appl. Phys. Lett.* 81 (2002) 3708.
3. FUKUMOTO, H.; MURAMATSU, Y.; YAMAMOTO, T.; YAMAGUCHI, J.; ITAKA, K.; KOINUMA, H. *Macromol. Rapid Commun.* 25 (2004) 196.
4. WESSLER, B.; JEHANNO, V.; ROSSNER, W.; MAIER, W. F. *Appl. Surface Sci.* 223 (2004) 30.
5. WEBER, W.H.; MAKER, P.D. *IEEE J. Quantum Elect.* QE10 (1974) 679.
6. EVANGELOU, E.K.; KONOFAOS, N.; THOMAS, C.B. *Philosophical Magazine B* 80 (2000) 395.
7. GREEN, M.A. *Solar Energy* 76 (2004) 3.
8. WANG, Y.; GU, D.H.; GAN, F.X. *Phys. Stat. Sol. A* 186 (2001) 71.
9. PIOT, O.; MALAURIE, A.; MACHET, J. *Thin Solid Films* 293 (1997) 124.
10. URBONAVICIUS, E.; PETNYCYTE, E.; GALDIKAS, A. *Vacuum* 53 (1999) 377.
11. WAGENDRISTEL, A.; WANG, Y. *An Introduction to Physics and Technology of Thin Films*, World Scientific, Singapore, (1994).

12. HIRATSUKA, R.S. (IN MEMORIAM); SANTILLI, C.V.; PULCINELLI, S.H. *Química Nova* 18 (1995) 171.
13. MATTHEWS, A. *J. Vac. Sci. Tech.* 21 (2003) S224.
14. ROSSNAGEL, S.M. *J. Vac. Sci. Tech.* 21 (2003) S74.
15. Model ST-Electron Beam Gun-Power Supply Instruction Manual, TFI TELEMARK, (1996).
16. Sycon Instruments STM – 100/MF – Users Manual, (1994).
17. RUBO, E.A.A.; OLIVEIRA, L.; SIU LI, M. *Rad. Eff. Def. Solids* 147 (1998) 83.
18. SILVA, J.R.; DE SOUZA, N.C.; DOS SANTOS JR, D.S.; DE VICENTE, F.S.; MARLETTA, A.; SIU LI, M.; OLIVEIRA JR, O.N.; GIACOMETTI, J.A. *Synthetic Metals* 137 (2003) 1477.
19. DE VICENTE, F.S.; DE CASTRO, A.C.; DE SOUZA, M.F.; SIU LI, M. *Thin Solid Films* 418 (2002) 222.
20. DE VICENTE, F.S.; SIU LI, M.; NALIN, M.; MESSADDEQ, Y. *J. Non-Cryst. Solids* 330 (2003) 168.
21. BERNARDI, M.I.B.; DE VICENTE, F.S.; MAIA, L.J.Q.; SIU LI, M.; HERNANDES, A.C. *Thin Sol. Films* (2003) (in press).
22. RUBO, E.A.A., PhD Thesis, Instituto de Física de São Carlos – USP (2000).
23. MENG, X.; NATANSOHN, A.; ROCHON, P. *J. Polym. Sci. Polym. Phys.* 34 (1996) 1461.
24. SEKKAT Z.; WOOD, J. *Synth. Met.* 81 (1996) 281.
25. DHANABALAN, A.; BALOGH, D.T.; CONSTANTINO, C.J.L.; RIUL JR., A.; OLIVEIRA JR., O.N.; GIACOMETTI, J.A. *Mater. Res. Symp. Proc.* 488 (1998) 927.
26. TAUNAUMANG, H.; HERNAN, M.O. *Optical Materials* 18 (2001) 343.
27. URLACHER, C.; MARCO DE LUCAS, C.; BERNESTEIN, E.; JACQUIER, B.; MUGNIER, J. *Optical Mater.* 12 (1999) 19.
28. REISFELD, R.; ZELNER, M.; PATRA, A. *J. Alloys Compounds* 300-301 (2000) 147.
29. YOSHIMURA, M. *Cer. Bull.* 67 (12) (1988) 1950.
30. TSENG, T.F.; YANG, C.C.; LIU, K.S.; WU, J.M.; WU, T.B.; LIN, I.N. *Jpn. J. Appl. Phys.* 35 (1996) 4743.
31. KIM, S.S.; KANG, T.S.; JE, J.H. *Thin Solid Films* 405 (2002) 117.